

# Measurement of nonlinear rheology of cross-linked biopolymer gels

Chase P. Broedersz,<sup>ab</sup> Karen E. Kasza,<sup>b</sup> Louise M. Jawerth,<sup>b</sup> Stefan Münster,<sup>bc</sup> David A. Weitz<sup>\*b</sup> and Frederick C. MacKintosh<sup>\*a</sup>

Received 23rd April 2010, Accepted 17th June 2010

DOI: 10.1039/c0sm00285b

One of the hallmarks of biopolymer gels is their nonlinear viscoelastic response to stress, making the measurement of the mechanics of these gels very challenging. Various rheological protocols have been proposed for this; however, a thorough understanding of the techniques and their range of applicability as well as a careful comparison between these methods are still lacking. Using both *strain ramp* and *differential prestress* protocols, we investigate the nonlinear response of a variety of systems ranging from extracellular fibrin gels to intracellular F-actin solutions and F-actin cross-linked with permanent and physiological transient linkers. We find that the prestress and strain ramp results agree well for permanently cross-linked networks over two decades of strain rates, while the protocols only agree at high strain rates for more transient networks. Surprisingly, the nonlinear response measured with the prestress protocol is insensitive to creep; although a large applied steady stress can lead to significant flow, this has no significant effect on either the linear or nonlinear response of the system. A simple model is presented to provide insight into these observations.

## Introduction

The mechanical properties of cells depend largely on their cytoskeleton, an intracellular network consisting of various biopolymers such as F-actin and associated proteins for cross-linking and stress generation. At a larger scale, most tissue cells are not viable when suspended in a fluid, but depend on the stiff anchorage provided by the extracellular matrix,<sup>1</sup> which also consists of filamentous protein polymers. Both intracellular and extracellular biopolymer networks exhibit remarkable mechanical properties, as demonstrated in numerous *in vitro* studies: their mechanical response is highly nonlinear, exhibiting both a pronounced elastic stiffening<sup>2–12</sup> and large, negative normal stress under applied shear.<sup>13–15</sup> This stiffening response is thought to moderate large deformations that endanger cellular and tissue integrity. However, during various essential cell functions such as crawling, invasion and division the cytoskeleton must remodel, while simultaneously buttressing against external stress. The combination of these seemingly incompatible properties poses a significant experimental challenge for quantitative measurement of biopolymer gel mechanics. Traditional rheological methods are not sufficient for such systems and new methods are needed.

In many soft matter systems, a nonlinear response arises under flow conditions in the form of shear thickening or thinning. By contrast, the nonlinear response of reconstituted cross-linked biopolymer networks is largely elastic in nature. Many physiological cross-links are not permanent, however, and their transient nature complicates the mechanical response by enabling stress

relaxation and network flow.<sup>16,17</sup> The typical unbinding time of a cross-linking protein for F-actin ranges from seconds to minutes;<sup>17–19</sup> thus cross-linker unbinding occurs on biological timescales and must be accounted for.<sup>45</sup> This suggests various problems for the commonly used protocols.<sup>2,3,20–22</sup> During a strain ramp, in which the strain is the control variable that is increased linearly in time while the stress is measured, the elastic response and stress relaxation occur together, leading to an inevitable rate dependence of the measured elasticity.<sup>20,23</sup> In a prestress measurement the stress is the control variable and an incremental response is measured in the presence of a constant applied prestress.<sup>3,24</sup> However, concerns have been raised that a steadily applied prestress could also induce flow or restructuring of the sample, which is expected to affect the material properties.<sup>20</sup> A thorough understanding of the various measurement techniques is crucial to quantitatively explore the nonlinear mechanical response of biopolymer gels. Furthermore, a careful comparison between these protocols is needed to determine which protocol is most suitable to accurately measure the nonlinear mechanical response for different systems.

Here we study the nonlinear response of biopolymer gels with the prestress protocol and make a comparison with strain ramps, which we perform over a broad range of strain rates. We further study how the large stresses applied in the prestress protocol on timescales of minutes affect both the linear and nonlinear elastic response as determined when the applied prestress is the control variable; simultaneously we monitor the creep. To explore the generality of our results we investigate a range of systems: F-actin solutions and F-actin cross-linked with biotin–NeutrAvidin permanent rigid cross-links or physiological linkers for which we use human filamin, a large flexible cross-linker. To extend the scope to extracellular fiber networks we also probe fibrin gels. The nonlinear response obtained with the prestress and strain ramp protocols agree well for permanent networks over two decades of strain rates. By contrast, the two protocols agree only at high strain rates for more transient networks. We further find

<sup>a</sup>Department of Physics and Astronomy, Vrije Universiteit, Amsterdam, The Netherlands. E-mail: fcm@nat.vu.nl

<sup>b</sup>Department of Physics and School of Engineering and Applied Sciences, Harvard University, 29, Oxford Street, Cambridge, MA, 02138, USA. E-mail: weitz@seas.harvard.edu

<sup>c</sup>Max Planck Institute for the Science of Light, Erlangen, Germany and Center for Medical Physics, and Technology, Universität Erlangen-Nürnberg, Erlangen, Germany

that the prestress protocol is insensitive to creep; even when the applied stress leads to significant accumulated strain, we observe no significant effect on both the linear and the nonlinear response of the system, and the nonlinear response does not evolve significantly over time. We propose a simple yet general material model that includes the nonlinear elasticity of the network as well as network flow on long timescales. This model can help to understand and account for our observations when applying the two different measurement protocols.

## Materials and methods

G-Actin is obtained from rabbit skeletal muscle and actin samples are prepared by mixing monomeric actin with solutions of 10× polymerization buffer (20 mM Tris–HCl, 20 mM MgCl<sub>2</sub>, 1 M KCl, 2 mM DTT, 2 mM CaCl<sub>2</sub>, 5 mM ATP and pH 7.5). The actin–filamin samples are prepared by gently mixing solutions of 10× polymerization buffer with a solution of recombinant human filamin A purified from Sf9 cell lysates and monomeric actin at a molar ratio of 0.003. For permanently cross-linked networks, biotinylated actin monomers are incorporated in actin filaments at a molar ratio of biotinylated monomers to non-biotinylated monomers  $R = 0.003$ . Cross-linking is mediated by NeutrAvidin proteins. Samples are prepared by mixing solutions of 10× polymerization buffer, biotinylated monomeric actin, and monomeric actin. After 3 minutes incubation, NeutrAvidin at a 1 : 1 molar ratio to biotinylated actin is gently mixed in.

Human fibrinogen (Enzyme Research Laboratories, South Bend, IN) is diluted in fibrin buffer (150 mM NaCl, 20 mM Tris, 20 mM CaCl<sub>2</sub> and pH 7.4) to a final concentration of 0.8 mg ml<sup>-1</sup>. Polymerization is initiated by addition of human  $\alpha$ -thrombin (Enzyme Research Laboratories, South Bend, IN) with a final concentration of 0.05 U ml<sup>-1</sup>. After addition of thrombin, samples are pipetted briefly to mix and immediately pipetted into the rheometer. The networks are allowed to polymerize for two hours before all rheological tests.

The mechanical response is measured with a stress-controlled rheometer (Ares G2, TA Instruments), using a 40 mm diameter stainless steel parallel plate geometry with a gap of 160  $\mu$ m for the actin samples and a 20 mm diameter stainless steel parallel plate with a gap of 500  $\mu$ m for the fibrin samples. All samples are polymerized *in situ* at 25 °C. We apply a thin layer of low viscosity mineral oil around the sample to minimize evaporation. Linear viscoelastic moduli are obtained by applying an oscillatory stress,  $\sigma(t) = \sigma e^{i\omega t}$ , and measuring the resulting strain,  $\gamma(t) = \gamma e^{i\omega t}$ ; the complex modulus  $G^* = G' + iG''$  is determined from  $G^* = \frac{\sigma}{\gamma}$ .

The nonlinear mechanical response is quantified using two distinct protocols. In the strain ramp protocol, the applied deformation of the sample is the control variable and the strain  $\gamma(t)$  is steadily increased at a fixed rate, while the resulting stress  $\sigma_t$  is measured. Both  $\sigma_t$  and  $\gamma(t)$  are smoothed using a cubic spline algorithm in Matlab to compute the differential modulus  $K = \frac{d\sigma}{d\gamma}$  by applying a numerical derivative to the stress–strain curve. By contrast, in the prestress protocol, the applied stress is the control variable and we perform differential measurements to determine the material's differential stiffness. A steady prestress,  $\sigma_0$ , is applied on which a small amplitude oscillatory stress,  $\delta\sigma(t) = \delta\sigma e^{i\omega t}$  is superposed at a frequency  $\omega$  of 6.3 rad s<sup>-1</sup>; we measure

the total strain and determine the small oscillatory strain response,  $\delta\gamma(t) = \delta\gamma e^{i\omega t}$ . The oscillatory stress amplitude used is at most 10% of the steady prestress, and we confirm that the response is linear in  $\delta\sigma$  for all  $\sigma_0$ . The complex differential or tangent viscoelastic modulus is determined from  $K^*(\omega, \sigma_0) = \frac{\delta\sigma}{\delta\gamma}$ .

## Results

### 1. Linear mechanical response

To characterize the systems, we measure the frequency dependence of the linear viscoelastic moduli. When 0.5 mg ml<sup>-1</sup> biotinylated actin (biotin : actin molar ratio of 0.003) is polymerized in the presence of NeutrAvidin it forms a soft, predominantly elastic gel. Within the frequency range we study here,  $G' \approx 1$  Pa and appears to be virtually independent of frequency, as shown in Fig. 1a. At a frequency of 0.1 Hz,  $G'$  is at least 10-fold smaller than  $G''$ . In the absence of cross-links polymerized actin forms an entangled solution. This soft viscoelastic material has an elastic modulus of only  $G' \approx 0.5$  Pa at a frequency of 0.1 Hz and  $G'$  is larger than  $G''$  (Fig. 1b). Consistent with previous studies,<sup>25–27</sup> both viscoelastic moduli exhibit a weak frequency dependence, as shown in Fig. 1b. Interestingly, when actin is polymerized in the presence of filamin (filamin : actin molar ratio of 0.003), the viscoelastic response changes only marginally as compared to the pure F-actin solution. Although the linear elastic modulus increases to  $G' = 1$  Pa, the  $G'$  to  $G''$  ratio remains small and the moduli still exhibit a weak frequency dependence, as shown in Fig. 1c. Thus, in contrast to permanent biotin–NeutrAvidin linking, the filamin cross-links form a gel with a considerable viscous component.

The polymerization of fibrinogen is initiated by the addition of thrombin, inducing the formation of a network of thick fiber bundles with diameters on the order of hundreds of nanometres.<sup>28</sup> The presence of fibronectin (FXIII) enzymatically promotes the formation of molecular bonds between protofibrils inside the bundle as well as between fiber bundles.<sup>29,30</sup> The fibrin gels are stiffer than the actin gels studied here and have an elastic shear modulus of  $G' = 16$  Pa, as shown in Fig. 1d. The elastic modulus  $G'$  is roughly 10-fold larger than  $G''$  and appears to be independent of frequency in the range we probed, consistent with previous experiments.<sup>31</sup> The viscous modulus  $G''$ , however, exhibits a pronounced minimum at a frequency of 0.03 Hz; this together with the subsequent increase of  $G''$  at lower frequencies may be indicative of a relaxation process at low frequencies.

### 2. Nonlinear response—strain ramp protocol

To quantify the nonlinear mechanical response we first employ the strain ramp protocol. In principle, this represents the most direct method to probe the stress–strain behavior of a material, since the stress is measured as a function of an applied strain that increases linearly with time. It has been reported that pure F-actin solutions exhibit a nonlinear response that depends strongly on the strain rate  $\dot{\gamma}$ .<sup>20</sup> By contrast, for actin networks with permanent biotin–NeutrAvidin cross-links the strain ramps exhibit no significant dependence on strain rate over two decades of  $\dot{\gamma}$ , as shown in Fig. 2a. Interestingly, the strain ramp measurements of F-actin networks cross-linked by filamin also depend strongly on  $\dot{\gamma}$ . The amount of stiffening becomes comparable to the biotin–NeutrAvidin

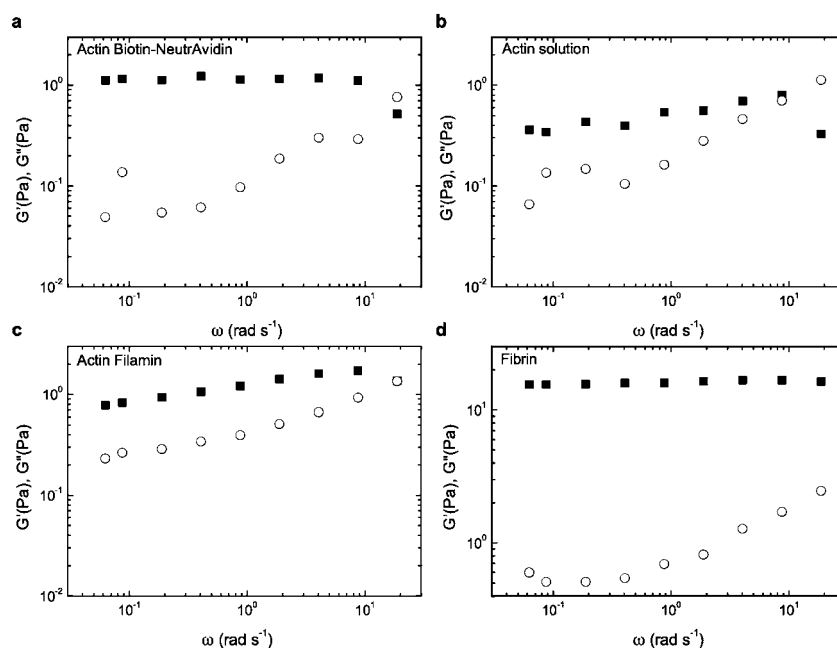


**Fig. 1** Linear rheology. The linear viscoelastic moduli  $G'$  (squares),  $G''$  (circles) as a function of frequency for (a) F-actin with a permanent biotin–NeutrAvidin cross-links. (b) F-Actin solution. (c) Actin cross-linked with the physiological linker protein filamin. (d) Fibrin with factor XIII.

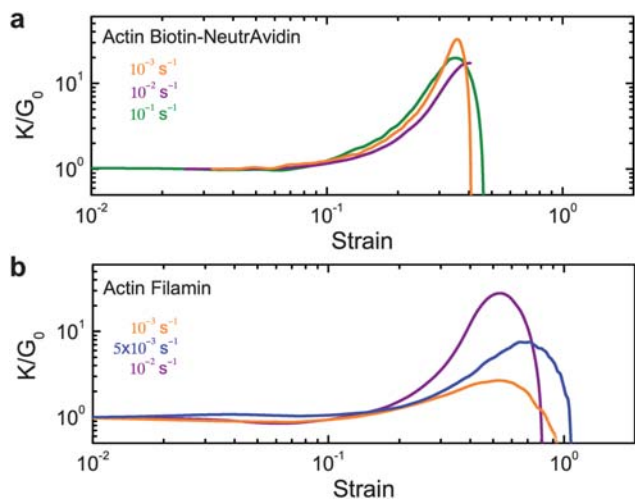


**Fig. 2** Strain ramp protocol. The tangent modulus  $K = d\sigma/d\gamma$  normalized by the linear modulus  $G_0$  as a function of strain for various strain rates  $\dot{\gamma}$ :  $10^{-3} \text{ s}^{-1}$  (orange),  $5 \times 10^{-3} \text{ s}^{-1}$  (blue),  $10^{-2} \text{ s}^{-1}$  (purple) and  $10^{-1} \text{ s}^{-1}$  (green). (a) F-Actin cross-linked with biotin–NeutrAvidin. (b) F-Actin cross-linked with filamin.

cross-linked actin only at strain rates as high as  $\dot{\gamma} = 0.01 \text{ s}^{-1}$ , as shown in Fig. 2b.

### 3. Nonlinear response—prestress protocol

We also characterize the nonlinear, differential mechanical properties of biopolymer gels with the prestress protocol. Small stress oscillations are superimposed on a constant stress  $\sigma_0$  to measure the elastic differential modulus  $K'$ ; the shear direction of the small stress oscillation is chosen to be along the same axis as the shear direction of the prestress.<sup>32</sup> To investigate the effect of the steady prestress on the linear and nonlinear mechanical

properties as well as on the deformation of the material we employ the following detailed protocol. Each prestress measurement is held for 4 minutes at positive shear alternated with 4 minutes without load and subsequently repeated at higher prestress magnitude. The total strain and  $K'$  are monitored continuously throughout this protocol. After reaching a maximum value in the applied prestress we follow the same procedure in reverse to study possible hysteresis. In this reverse protocol the prestresses are applied in the same (positive) shear direction as in the forward protocol.

Both in permanent F-actin networks with biotin–NeutrAvidin cross-links as well as in pure F-actin solutions,  $K'$  responds to an applied prestress by a rapid increase, after which it exhibits no time-dependence, as shown in the lower panels of Fig. 3a and b. In the actin–filamin and fibrin systems, however,  $K'$  shows a relatively slower response to a step in the applied prestress (lower panel Fig. 3c–e), although  $K'$  does appear to level off to a time-independent value. At the largest prestresses though this leveling off appears to occur more slowly. For the fibrin system we performed the same protocol with 16 minute prestress pulses and found that  $K'$  does level off within 16 minutes for prestresses as large as 40 Pa (data not shown). Remarkably, for all systems we observe that the mechanical response rapidly relaxes to the initial linear modulus as soon as the prestress is removed, unless the material breaks as demonstrated for an F-actin solution in the lower panel of Fig. 3b. We note that in the prestress protocol the materials state of stress is the control variable and unloading of the sample might result in a deformed state different from the initial one. However, the experiments here show that the linear mechanical properties measured at that unloaded state are unaffected by the previously applied large prestresses, even for large prestress to which the system responds nonlinearly.

To investigate to what extent the prestress affects the nonlinear mechanical properties, we reverse the protocol, moving from

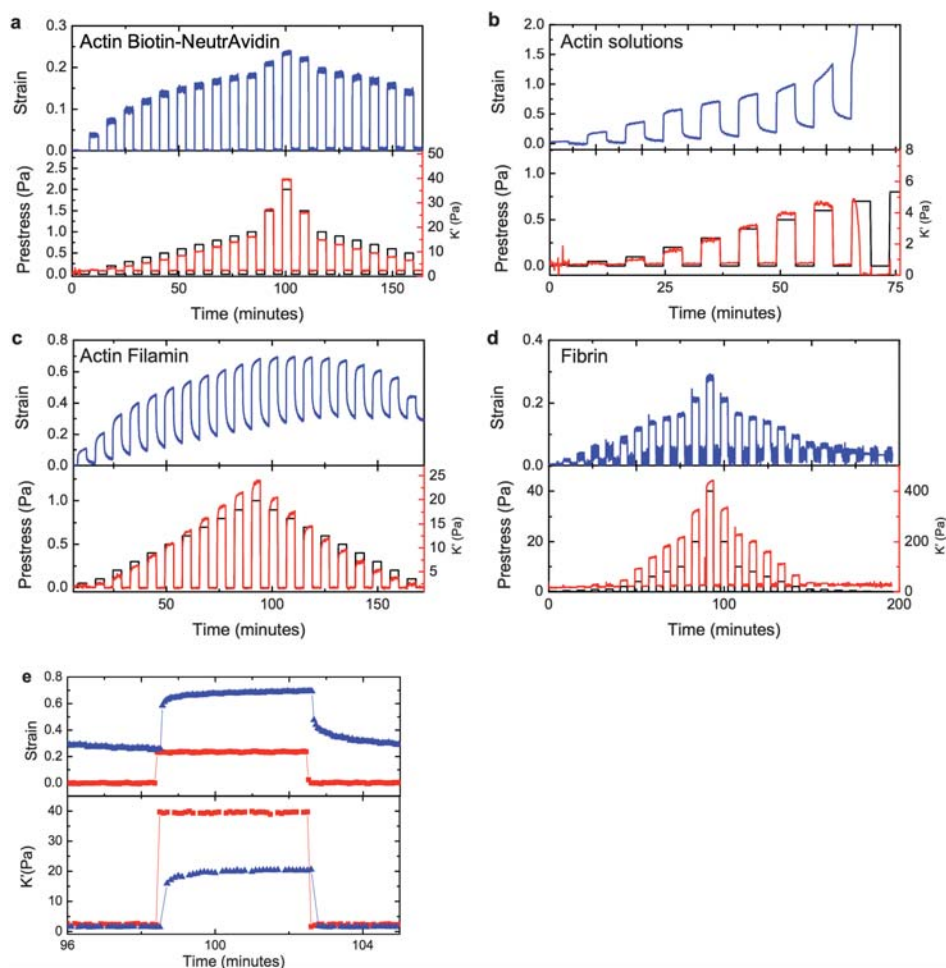


**Fig. 3** Prestress protocol. The strain (blue curves) and the differential modulus  $K'$  (red curves) as a function of time during 4 minute prestress pulses (black curves) applied every 4 minutes of increasing and then decreasing magnitude. (a) F-Actin with permanent biotin–NeutrAvidin cross-links. (b) F-Actin solution. (c) Actin cross-linked with the physiological linker protein filamin. (d) Fibrin with factor XIII. (e) Close-up of the strain and differential modulus  $K'$  during the 13<sup>th</sup> prestress pulse of 2 Pa for actin with NeutrAvidin (red squares) and with a prestress of 2 Pa for actin with filamin (blue triangles).

high to low prestress magnitude, after reaching the largest applied prestress. A potentially large effect could be anticipated in the cross-linked systems, since the applied prestress could lead to forced cross-link unbinding. Surprisingly, we observe no significant hysteresis for the cross-linked actin systems as well as for the fibrin gels, as demonstrated by Fig. 3a, c and d. This observation indicates that, similar to the linear response, the nonlinear mechanical properties of these systems determined at a prescribed prestress are unaffected by large prestresses applied over several minutes.

The absence of hysteresis effects might be particularly surprising in the more transient actin–filamin network. The relatively large viscous component as well as the significant frequency dependence of the shear moduli (Fig. 1c) imply flow on long timescales. To investigate this flow we monitor the creep for all systems during the entire prestress protocol. As expected, the more permanent actin biotin–NeutrAvidin and fibrin systems accumulate little or no strain during the entire protocol (Fig. 5a). By contrast, both the pure F-actin and actin–filamin gels exhibit a significant accumulation of strain; this indicates that the sample is plastically flowing.

The robustness of both the linear and nonlinear mechanical properties as measured with the prestress protocol in the presence of significant plastic flow is unexpected.

#### 4. Protocol comparison

We further make a side-by-side comparison between the prestress measurements and the strain ramps at various strain rates. The prestress method measures the nonlinear mechanical response at a specific frequency, while the strain ramp probes the system at a specific rate, and it thus probes the response over a range of frequencies. For a system with a broad and flat elastic plateau, however, this difference is not expected to be significant. For actin networks cross-linked with the permanent biotin–NeutrAvidin links and the fibrin gels we find excellent agreement between the two protocols over two decades of strain rates, as shown in Fig. 4 a and d. By contrast, for the actin–filamin system the strain ramp results exhibit a pronounced rate dependence (Fig. 4c). Interestingly, at large strain rates the strain-ramp results do show good agreement with the prestress results. For all systems we show both

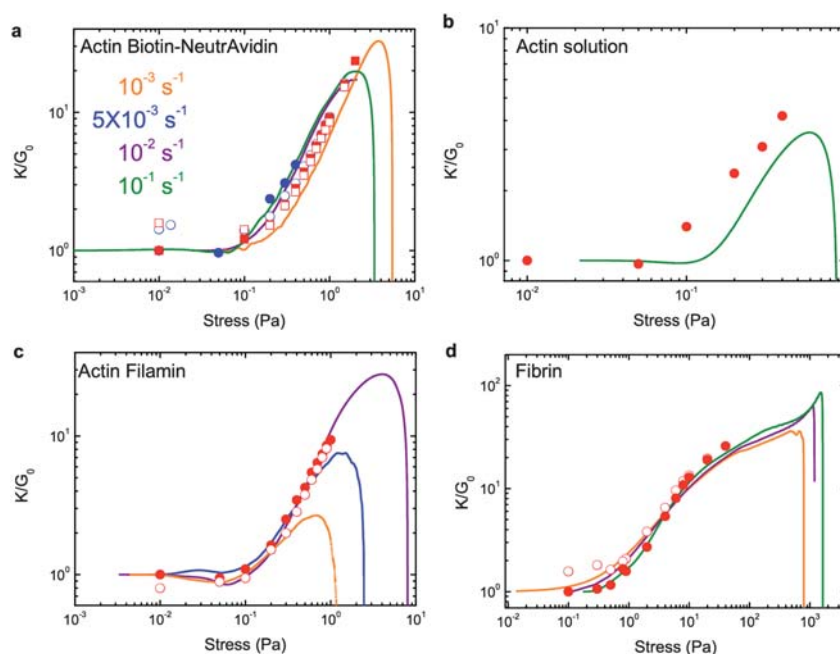


**Fig. 4** Protocol comparison. The tangent modulus (strain ramps) and differential modulus (prestress method)  $K$  normalized by the linear modulus  $G_0$  as a function stress  $\sigma$  (solid lines) for the prestress protocol with increasing prestress magnitude (closed symbols) and decreasing prestress magnitude (open symbols), and for the strain ramp protocol for various strain rates  $\dot{\gamma}$ :  $10^{-3} \text{ s}^{-1}$  (orange),  $5 \times 10^{-3} \text{ s}^{-1}$  (blue),  $10^{-2} \text{ s}^{-1}$  (purple) and  $10^{-1} \text{ s}^{-1}$  (green). (a) F-Actin with a permanent biotin–NeutrAvidin cross-links. (b) F-Actin solution. (c) Actin cross-linked with the physiological linker protein filamin. (d) Fibrin with factor XIII.

the prestress results using increasing levels of prestress (closed symbols) together with the results obtained after this by using decreasing levels of prestress (open symbols). In all cases, even for the actin–filamin gels that exhibit significant creep, we find no significant hysteresis.

## 5. Simple model

To gain insight into the nonlinear rheological behavior of cross-linked biopolymer gels we propose a simple model that captures the main features observed experimentally. The nonlinear mechanical properties can arise through a variety of mechanisms, ranging from the nonlinear entropic elasticity of single polymer segments between rigid cross-links in F-actin<sup>2,3,33</sup> and intermediate filament<sup>4,34,35,46</sup> networks, to the nonlinear response of the cross-links themselves, in the case of actin–filamin networks.<sup>36–40</sup> In other systems, the nonlinear elasticity may be due to non-affine deformations.<sup>5,41–43,13</sup> For the sake of generality of the model we do not make any assumptions about the underlying microscopic mechanism of strain stiffening. We do assume, however, that the elastic stiffness of the network responds instantaneously to an applied stress. Within this quasistatic approximation, the elastic stiffness of the network only depends on the current state of stress  $k = k(\sigma)$ . This approximation is easily justified on the long time-scales accessible by macrorheology for systems governed by the entropic elasticity of individual polymer segments. An applied tension extends a thermally contracted polymer strand; after a sufficiently large tension is applied, the entropic stiffness of this segment relaxes to a new increased equilibrium value. The time-scale for this process depends on the relaxation times of the thermally driven transverse fluctuations of the polymer segment.

For a typical cross-linked F-actin network this relaxation time can be estimated to be on the order of milliseconds<sup>44</sup> and can thus be considered instantaneous on the much longer timescales we probe with macrorheology. Even for non-affinely deforming networks, in which the nonlinearity can be associated with the buckling of filaments<sup>6,13,42</sup> this quasistatic approximation can be expected to be valid, provided that the spatial extent of such buckling is not too large.

In a transiently cross-linked network, the macroscopic strain is shared between two modes of deformation  $\gamma = \gamma_e + \gamma_f$ ; the first mode  $\gamma_e$  consists of the reversible deformation of the network, whereas the second mode of deformation  $\gamma_f$  captures the flow of the network itself. Assuming that the strains in these two components are additive is equivalent to assuming that the stresses are always equal,  $\sigma_e = \sigma_f = \sigma$ . It is convenient to set up a theoretical description of the *nonlinear* mechanical properties in terms of relations between small changes in stress  $d\sigma = \frac{d\sigma}{dt} dt$  and the corresponding small changes in the strain  $d\gamma = \frac{d\gamma}{dt} dt$ . The reversible deformation of the network is described by a simple nonlinear viscoelastic model in which the elasticity  $k(\sigma)$  and viscosity  $\eta$  contribute to the stress in parallel

$$\frac{d\sigma}{dt} = \left[ k(\sigma) + \eta \frac{d}{dt} \right] \frac{d\gamma_e}{dt}. \quad (1)$$

The long-time flow of the network enables stress-relaxation. This relaxation may in general be governed by a spectrum of relaxation times.<sup>45</sup> For simplicity, we here use a minimalistic approach that considers only a single relaxation timescale, although the main qualitative behavior of this model does not

depend on this assumption. In practice, this assumption implies that we treat the long-time flow of the network as a simple liquid with a viscosity  $\zeta \gg \eta$ , for which the stress relaxation is given by

$$\frac{d\sigma}{dt} = \zeta \frac{d^2\gamma_f}{dt^2}. \quad (2)$$

Eqn (1) and (2) together describe the rheological behavior of this model. Eqn (1) can also be understood as a nonlinear generalization of the Kelvin–Voigt model in which a dashpot is placed parallel to a nonlinear spring, while eqn (2) describes a Newtonian liquid-like stress relaxation. Equating the stresses represented in eqn (1) and (2) amounts to the assumption that the strain of the system has two contributions with additive compliance. This can also be understood as a second dashpot that is placed in series with the nonlinear Kelvin–Voigt element. Such a construction allows any stress stored in the spring to completely relax on long timescales at constant total strain. This addition to the Kelvin–Voigt element is essential for transient systems in which the stress can largely relax on long timescales.<sup>16,17,19</sup>

In the prestress protocol a time-independent prestress  $\sigma_0$  is imposed together with a small oscillatory stress  $\delta\sigma(t)$  such that  $\sigma(t) = \sigma_0 + \delta\sigma(t)$  and the resulting strain response  $\gamma(t)$  is measured. This strain response can be decomposed as  $\gamma(t) = \gamma_0(t) + \delta\gamma(t)$ , where  $\gamma_0(t)$  is the time-dependent creep response and  $\delta\gamma(t)$  is a small-amplitude oscillatory strain, as illustrated in the inset of Fig. 5a. After an applied steady stress,  $\gamma_0(t)$  increases rapidly after which it asymptotically approaches a regime in which  $\gamma_0(t) \sim t$ . Symmetry considerations imply that the network stiffness should be an even function of  $\sigma$ , and therefore to linear order  $k(\sigma) = k(\sigma_0)$ . Thus, for the prestress protocol eqn (1) and (2) yield

$$\begin{aligned} \sigma_0 + \delta\sigma &= \left[ k(\sigma_0) + \eta \frac{d}{dt} \right] \gamma_{0e} + \left[ k(\sigma_0) + \eta \frac{d}{dt} \right] \delta\gamma_e \\ &= \zeta \frac{d}{dt} \gamma_{0f} + \zeta \frac{d}{dt} \delta\gamma_f, \end{aligned} \quad (3)$$

where  $\gamma_0 = \gamma_{0e} + \gamma_{0f}$  and  $\delta\gamma_0 = \delta\gamma_{0e} + \delta\gamma_{0f}$ . The creep strain  $\gamma_0$  consists of both the network ( $\gamma_{0e}$ ) and flow ( $\gamma_{0f}$ ) response to a constant stress. After an initial relaxation, the former is expected to approach a constant, while the latter increases linearly with time. Remarkably, the differential components of the stress and strain are decoupled from the steady stress and creep strain in eqn (3). This decoupling allows for a measurement of the differential response in parallel to a steady prestress, even when the sample is creeping. This result also holds when the long-time flow of the network is characterized by a spectrum of timescales. The in-phase differential response to an oscillatory stress is given by

$$K'(\omega) = k(\sigma_0) \frac{1}{\left(1 + \frac{\eta}{\zeta}\right)^2 + \left(\frac{k}{\zeta\omega}\right)^2}. \quad (4)$$

At high frequencies there is a plateau  $K' = k(\sigma_0) \frac{1}{(1 + \eta/\zeta)^2} \approx k(\sigma_0)$ .

To demonstrate that this model qualitatively captures the experimentally observed strain response (upper panels, Fig. 3), we compute the creep response to a series of increasing stress pulses alternated with zero stress periods, and its reverse order, as

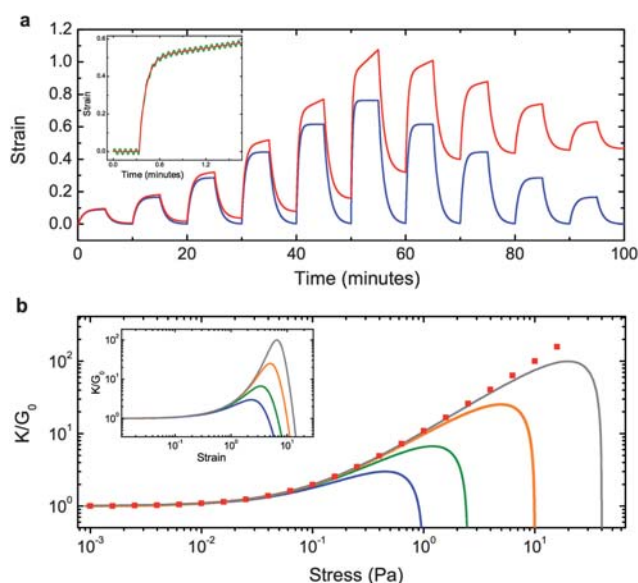


**Fig. 5** Model. (a) The calculated strain as a function of time during 4 minute prestress pulses applied every 4 minutes of increasing and then decreasing magnitude for a network ( $\eta = 60$  Pa s,  $k_0 = 1$  Pa,  $k_1 = 0.6$ , see main text) that is transient (red curve) and exhibits long-time flow ( $\zeta = 6000$  Pa s), and a network that is permanent ( $\zeta \rightarrow \infty$ , blue curve). The inset shows the strain response  $\gamma(t) = \gamma_0(t) + \delta\gamma(t)$  (green line) and the creep response  $\gamma_0(t)$  (red line) to an applied steady stress superposed on a small oscillatory stress. (b) The calculated differential modulus as a function of stress for the prestress protocol (symbols) and the strain ramp protocol (solid lines with strain rates  $10^{-3}$  s $^{-1}$ ,  $5 \times 10^{-3}$  s $^{-1}$ ,  $10^{-2}$  s $^{-1}$  and  $5 \times 10^{-2}$  s $^{-1}$  increasing from blue to gray). The inset shows the differential modulus as a function of strain for the strain ramp protocol.

in the experimentally used protocol. For this calculation an interpolation formula is used for the dependence of the differential elastic stiffness  $\sigma(k) \approx k_0 + k_1\sigma$ , (with  $\sigma > 0$ ) appropriate for an actin–filamin gel.<sup>36–38</sup> We find that during a prestress protocol strain accumulates, as depicted as a red line in Fig. 5a. Interestingly, the calculated response exhibits a remarkable resemblance with the creep response for the actin–filamin system (upper panel, Fig. 3c). Permanent cross-links, however, inhibit network flow  $\zeta \rightarrow \infty$ , and as a result there is no strain accumulation during the prestress protocol in such a permanent network, as shown as a blue line in Fig. 5a. This is consistent with the experimental behavior we observe for F-actin networks with biotin–NeutrAvidin cross-links and fibrin (upper panel, Fig. 3a and d).

To address the general nonlinear rheological response of this model we combine eqn (1) and (2) to obtain

$$\begin{aligned} \left(1 + \frac{\eta}{\zeta}\right) \frac{d^2\sigma}{dt^2} + \frac{k(\sigma)}{\zeta} \left(1 - (\eta + \zeta) \frac{d}{dt} \frac{k(\sigma)}{k(\sigma)^2}\right) \frac{d\sigma}{dt} \\ = k(\sigma) \left(1 - \eta \frac{d}{dt} \frac{k(\sigma)}{k(\sigma)^2}\right) \frac{d^2\gamma}{dt^2} + \eta \frac{d^3\gamma}{dt^3} \end{aligned} \quad (5)$$

The initial conditions required to solve this differential equation can be found by inspecting the zero-stress linear limit of the model, in which  $\frac{k}{\zeta}\sigma + (1 + \eta/\zeta)\frac{d\sigma}{dt} = k(\sigma=0)\frac{d\gamma}{dt} + \eta\frac{d^2\gamma}{dt^2}$ . For instance, in the case of a strain ramp the right hand side of eqn (5) vanishes and the initial conditions become

$\sigma(0) = 0$  Pa,  $\left. \frac{d\sigma}{dt} \right|_{t=0} = \frac{k(\sigma = 0 \text{ Pa})}{1 + \eta/\zeta} \frac{dy}{dt}$ . The calculated response to a strain ramp at a variety of strain rates is shown in Fig. 5b. Beyond a characteristic value for  $\sigma$ ,  $K$  increases strongly with the applied stress. Interestingly, at slower strain rates the dependence of  $K$  with  $\sigma$  is weaker, while at large strain rates the response converges to a curve in which at large stresses  $K \sim \sigma$ , as can be expected for the nonlinear network elasticity we assumed for this example. Consistent with the measured behavior (Fig. 4), the high strain-rate limit curve coincides with the response as measured with a prestress protocol, as shown in Fig. 5b. At very high strain rates the quasistatic approximation will break down. In that case the strain ramp results can be expected to exceed the prestress results. Such high strain rates are, however, not accessible by most rheometers.

## Discussion and implications

We have studied the nonlinear mechanical response of a range of biopolymer gels with both the strain ramp and the prestress protocols. The prestress and strain ramp results agree well over two decades in strain rate for biotin–NeutrAvidin cross-linked F-actin networks and cross-linked fibrin networks. For networks exhibiting creep such as the actin–filamin system, however, the two protocols agree only at high strain rates. The discrepancy in the results of the prestress and low-rate strain ramp protocols can be accounted for by the mode of stress relaxation in these systems; both the high-rate strain ramp and prestress protocols measure the fast nonlinear elastic response, while at low rates the stress measured during a strain ramp is the relatively fast elastic response convoluted with stress relaxation processes. These stress relaxation processes can be enabled by cross-linker unbinding events. Although, the rates of such cross-linker unbinding events can be force-dependent,<sup>23,36</sup> this is not required to explain the experimental behavior we observe here.

We have developed a simple model, which accounts for the experimentally observed behavior. It captures the general nonlinear elastic response of a cross-linked biopolymer network, while allowing for simple flow of the network on long timescales. This model illustrates how the differential non-linear elastic response can be measured with the prestress protocol, even while the system is creeping. A microscopic description of the long-time network flow is required to expand this model as to provide a quantitative description for the nonlinear rheology of cross-linked biopolymer gels.

It is important to monitor the strain during the prestress measurement to determine the extent of creep. Surprisingly, for systems that exhibit creep, the prestress method consistently yields results insensitive to this creep. By contrast, for the strain ramp technique, the elastic response and the creep are fundamentally coupled and cannot be separated because strain is the control variable; the results obtained with this technique are difficult to interpret for systems that creep. Thus, for systems that exhibit creep, the prestress method shows a clear advantage over the strain ramp method.

The prestress method is designed to quantify the nonlinear response of viscoelastic solids. This method, however, may not always be suitable for systems that exhibit a significant amount of creep; the flow induced by a steady stress can lead to

restructuring, which might in turn affect the mechanical properties of the system. In this paper we have discussed a detailed protocol to test the applicability of the prestress method for a particular system. For all systems investigated here, the repeated large steady stresses applied over 4 minutes during the prestress protocol do not significantly affect either the linear or the nonlinear elastic properties; as measured with differential prestress experiments, the mechanical properties exhibit no significant time evolution, even if there is considerable creep. The results presented here demonstrate conclusively that the prestress method is a robust and reliable method for measuring the nonlinear viscoelastic properties biopolymer gels, even for systems that exhibit creep.

## Acknowledgements

This work was supported in part by FOM/NWO and by the NSF (DMR-0602684) and the Harvard MRSEC (DMR-0213805). CPB acknowledges the hospitality of Harvard University where the experimental part of this work was performed. We thank F. Nakamura for the gift of actin and filamin protein.

## References

- 1 A. L. Zajac and D. E. Discher, *Curr. Opin. Cell Biol.*, 2008, **20**, 609–615.
- 2 C. Storm, J. J. Pastore, F. C. MacKintosh, T. C. Lubensky and P. A. Janmey, *Nature*, 2005, **435**, 191–194.
- 3 M. L. Gardel, J. H. Shin, F. C. MacKintosh, L. Mahadevan, P. Matsudaira and D. A. Weitz, *Science*, 2004, **304**, 1301–1305.
- 4 Y.-C. Lin, N. Y. Yao, C. P. Broedersz, H. Herrmann, F. C. MacKintosh and D. A. Weitz, *Phys. Rev. Lett.*, 2010, **104**, 058101.
- 5 O. Lieleg, M. M. A. E. Claessens, C. Heussinger, E. Frey and A. R. Bausch, *Phys. Rev. Lett.*, 2007, **99**, 088102–088104.
- 6 O. Chaudhuri, S. H. Parekh and D. A. Fletcher, *Nature*, 2007, **445**, 295–298.
- 7 I. K. Piechocka, M. Bacabac, M. Potters, F. C. MacKintosh and G. H. Koenderink, *Biophys. J.*, 2010, **98**, 2281.
- 8 K. E. Kasza, A. C. Rowat, J. Liu, T. E. Angelini, C. P. Brangwynne, G. H. Koenderink and D. A. Weitz, *Curr. Opin. Cell Biol.*, 2007, **19**, 101–107.
- 9 A. R. Bausch and K. Kroy, *Nat. Phys.*, 2006, **2**, 231–238.
- 10 J. Xu, Y. Tseng and D. Wirtz, *J. Biol. Chem.*, 2000, **275**, 35886–35892.
- 11 A. E. X. Brown, R. I. Litvinov, D. E. Discher, P. K. Purohit and J. W. Weisel, *Science*, 2009, **325**, 741–744.
- 12 P. A. Janmey, S. Hvidt, J. Lamb and T. P. Stossel, *Nature*, 1990, **345**, 89–92.
- 13 E. Conti and F. C. MacKintosh, *Phys. Rev. Lett.*, 2009, **102**, 088102.
- 14 P. A. Janmey, M. E. McCormick, S. Rammensee, J. L. Leight, P. C. Georges and F. C. MacKintosh, *Nat. Mater.*, 2007, **6**, 48–51.
- 15 H. Kang, Q. Wen, P. A. Janmey, J. X. Tang, E. Conti and F. C. MacKintosh, *J. Phys. Chem. B*, 2009, **113**, 3799–3805.
- 16 O. Lieleg, M. M. A. E. Claessens, Y. Luan and A. R. Bausch, *Phys. Rev. Lett.*, 2008, **101**, 108101–108104.
- 17 S. M. Volkmer Ward, A. Weins, M. R. Pollak and D. A. Weitz, *Biophys. J.*, 2008, **95**, 4915–4923.
- 18 H. Miyata, R. Yasuda and K. Kinoshita, *Biochim. Biophys. Acta, Gen. Subj.*, 1996, **1290**, 83–88.
- 19 D. Wachsstock, W. Schwarz and T. Pollard, *Biophys. J.*, 1994, **66**, 801–809.
- 20 C. Semmrich, R. J. Larsen and A. R. Bausch, *Soft Matter*, 2008, **4**, 1675–1680.
- 21 R. H. Ewoldt, A. E. Hosoi and G. H. McKinley, *J. Rheol. (Melville, NY, U. S.)*, 2008, **52**, 1427–1458.
- 22 R. H. Ewoldt, A. E. Hosoi and G. H. McKinley, *Integr. Comp. Biol.*, 2009, **49**, 40–50.
- 23 O. Lieleg and A. R. Bausch, *Phys. Rev. Lett.*, 2007, **99**, 158105.

- 24 M. L. Gardel, J. H. Shin, F. C. MacKintosh, L. Mahadevan, P. A. Matsudaira and D. A. Weitz, *Phys. Rev. Lett.*, 2004, **93**, 188102.
- 25 B. Hinner, M. Tempel, E. Sackmann, K. Kroy and E. Frey, *Phys. Rev. Lett.*, 1998, **81**, 2614.
- 26 M. L. Gardel, M. T. Valentine, J. C. Crocker, A. R. Bausch and D. A. Weitz, *Phys. Rev. Lett.*, 2003, **91**, 158302.
- 27 G. H. Koenderink, M. Atakhorrami, F. C. MacKintosh and C. F. Schmidt, *Phys. Rev. Lett.*, 2006, **96**, 138307-4.
- 28 E. Distasio, *Biophys. J.*, 1998, **75**, 1973–1979.
- 29 G. W. Nelb, C. Gerth and J. D. Ferry, *Biophys. Chem.*, 1976, **5**, 377–387.
- 30 C. Gerth, W. W. Roberts and J. D. Ferry, *Biophys. Chem.*, 1974, **2**, 208–217.
- 31 W. W. Roberts, O. Kramer, R. W. Rosser, F. Henry, M. Nestler and J. D. Ferry, *Biophys. Chem.*, 1974, **1**, 152–160.
- 32 J. Vermant, L. Walker, P. Moldenaers and J. Mewis, *J. Non-Newtonian Fluid Mech.*, 1998, **79**, 173–189.
- 33 F. C. MacKintosh, J. Käs and P. A. Janmey, *Phys. Rev. Lett.*, 1995, **75**, 4425.
- 34 N. Y. Yao, C. P. Broedersz, Y. C. Lin, K. E. Kasza, F. C. MacKintosh and D. A. Weitz, *Biophys. J.*, 2010, **98**, 2147.
- 35 S. Rammensee, P. A. Janmey and A. R. Bausch, *Eur. Biophys. J.*, 2007, **36**, 661–668.
- 36 K. E. Kasza, G. H. Koenderink, Y. C. Lin, C. P. Broedersz, W. Messner, F. Nakamura, T. P. Stossel, F. C. MacKintosh and D. A. Weitz, *Phys. Rev. E: Stat., Nonlinear, Soft Matter Phys.*, 2009, **79**, 041928; K. E. Kasza, C. P. Broedersz, G. H. Koenderink, Y. C. Lin, W. Messner, E. A. Millman, F. Nakamura, T. P. Stossel, F. C. MacKintosh and D. A. Weitz, *Biophys. J.*, in press.
- 37 C. P. Broedersz, C. Storm and F. C. MacKintosh, *Phys. Rev. E: Stat., Nonlinear, Soft Matter Phys.*, 2009, **79**, 061914.
- 38 C. P. Broedersz, C. Storm and F. C. MacKintosh, *Phys. Rev. Lett.*, 2008, **101**, 118103.
- 39 M. L. Gardel, F. Nakamura, J. H. Hartwig, J. C. Crocker, T. P. Stossel and D. A. Weitz, *Proc. Natl. Acad. Sci. U. S. A.*, 2006, **103**, 1762–1767.
- 40 B. Wagner, R. Tharmann, I. Haase, M. Fischer and A. R. Bausch, *Proc. Natl. Acad. Sci. U. S. A.*, 2006, **103**, 13974–13978.
- 41 C. Heussinger and E. Frey, *Phys. Rev. Lett.*, 2006, **97**, 105501.
- 42 P. R. Onck, T. Koeman, T. van Dillen and E. van der Giessen, *Phys. Rev. Lett.*, 2005, **95**, 178102.
- 43 E. M. Huisman, T. van Dillen, P. R. Onck and E. van der Giessen, *Phys. Rev. Lett.*, 2007, **99**, 208103.
- 44 F. Gittes and F. C. MacKintosh, *Phys. Rev. E: Stat. Phys., Plasmas, Fluids, Relat. Interdiscip. Top.*, 1998, **58**, R1241.
- 45 C. P. Broedersz, M. Depken, N. Y. Yao, M. R. Pollak, D. A. Weitz and F. C. MacKintosh, 2010, arXiv:1006.3940v2 [cond-mat.soft].
- 46 Y. C. Lin, C. P. Broedersz, A. C. Rowat, T. Wedig, H. Hermann, F. C. MacKintosh and D. A. Weitz, *J. Mol. Biol.*, 2010, **399**, 637.